第 58 卷 第 4 期
2025 年（总 242 期）

西 北 地 质
NORTHWESTERN GEOLOGY

Vol. 58 No. 4
2025（Sum242）

引文格式：周国超，王玉往，王京彬，等. 新疆东天山月牙湾铜镍硫化物矿床 Sr-Nd-Pb-S 同位素特征及其地质意义[J]. 西北地质，2025，58(4)：87−101. DOI：10.12401/j.nwg.2024088

Citation: ZHOU Guochao, WANG Yuwang, WANG Jingbin, et al. Sr-Nd-Pb-S Isotopic Characteristics and Its Geological Significance of the Yueyawan Cu-Ni Sulfide Deposit in East Tianshan, Xinjiang[J]. Northwestern Geology, 2025, 58(4): 87−101. DOI: 10.12401/j.nwg.2024088

新疆东天山月牙湾铜镍硫化物矿床 Sr-Nd-Pb-S 同位素特征及其地质意义

周国超[1]，王玉往[2]，王京彬[3]，石煜[4]，解洪晶[2]，李德东[2]，程先锋[1]

（1. 云南国土资源职业学院，云南 昆明 652501；2. 北京矿产地质研究院有限责任公司，北京 100012；3. 中色紫金地质勘查（北京）有限责任公司，北京 100012；4. 东华理工大学，核资源与环境国家重点实验室，江西 南昌 330013）

摘 要：新疆东天山地区是中国重要的铜镍成矿带，但其含矿岩体的岩浆起源和硫饱和机制存在较大争议，大南湖岛弧带内新发现的月牙湾铜镍硫化物为厘清这些争议提供了新的窗口。月牙湾岩体是多期次岩浆侵位形成的复式岩体，第一期岩浆作用形成辉长岩、橄长岩和橄榄辉长岩，第二期岩浆作用形成基性程度更高的暗色细粒橄榄辉长岩和暗色细粒橄长岩，是主要的赋矿岩相。岩石具有低($^{87}Sr/^{86}Sr$)$_i$(0.703 3～0.703 48)，高$\varepsilon_{Nd}(t)$(6.54～8.35)和Pb 同位素比值较低(($^{206}Pb/^{204}Pb$)$_i$=17.828～18.014，($^{207}Pb/^{204}Pb$)$_i$=15.446～15.478，($^{208}Pb/^{204}Pb$)$_i$=37.495～37.698)的特征，指示月牙湾岩体的形成与塔里木大火成岩省并无直接联系，而是源自亏损地幔，并且受到俯冲物质的交代。硫化物原位$\delta^{34}S$为 0.03‰～4.09‰，与卡拉塔格地区石炭纪—二叠纪围岩地层$\delta^{34}S$范围一致，表明在成矿过程中有地壳硫的加入。大南湖岛弧带的镁铁−超镁铁质岩体与康古尔剪切带和中天山地块中的镁铁−超镁铁质岩体具有相似的成岩时代和地球化学特征，剥蚀程度较浅，说明大南湖岛弧带具有较好的铜镍成矿潜力。

关键词：岩浆源区；硫饱和机制；同位素；月牙湾矿床；东天山

中图分类号：P597；P611 **文献标志码：**A **文章编号：**1009-6248(2025)04-0087-15

Sr-Nd-Pb-S Isotopic Characteristics and Its Geological Significance of the Yueyawan Cu-Ni Sulfide Deposit in East Tianshan, Xinjiang

ZHOU Guochao[1], WANG Yuwang[2], WANG Jingbin[3], SHI Yu[4], XIE Hongjing[2], LI Dedong[2], CHENG Xianfeng[1]

(1. Yunnan Land and Resources Vocational College, Kunming 652501, Yunnan, China; 2. Beijing Institute of Geology for Mineral Resources Co. Ltd., Beijing 100012, China; 3. Sino-Zijin Resources Ltd., Beijing 100012, China; 4. State Key Laboratory of Nuclear Resources and Environment, East China University of Technology, Nanchang 330013, Jiangxi, China)

Abstract: The East Tianshan orogenic belt is an important Cu-Ni sulfide mineralization belt in China. However, the mantle source and sulfur saturation mechanism are still controversial. The newly discovered Yuyawan Cu-

收稿日期：2023-10-30；**修回日期：**2024-07-25；**责任编辑：**曹佰迪

基金项目：国家重点研发计划项目子课题“幔源岩浆型成矿系统三维机构与矿体定位机制”(2017YFC0601204)资助。

作者简介：周国超(1989−)，男，博士，讲师，主要从事幔源岩浆成岩与成矿作用研究。E-mail：guochaozhou2008@126.com。

Ni sulfide deposit in the Dananhu arc provides a new target for these issues. The Yueyawan intrusion formed by two intrusive phases: the phase I is composed of gabbro, troctolite and olivine gabbro, and the phase II is composed of fine-grained olivine gabbro and fine-grained troctolite. The phase II rocks primarily contained sulfides. The rocks have low $(^{87}Sr/^{86}Sr)_i$ (0.703 3～0.703 48), high $\varepsilon Nd(t)$ (6.54～8.35) and low Pb isotopic ratios ($(^{206}Pb/^{204}Pb)_i$=17.828～18.014, $(^{207}Pb/^{204}Pb)_i$=15.446～15.478, $(^{208}Pb/^{204}Pb)_i$=37.495～37.698), indicating that the Yueyawan intrusion is not directly related to the Tarim Large Igneous Province, but originated from the depleted mantle and was replaced by subduction materials. The $\delta^{34}S$ of sulfide ranges from 0.03‰ to 4.09‰, which is consistent with the $\delta^{34}S$ of Carboniferous and Permian strata in Karatag area, indicating the addition of sulfur in the crust during the mineralization process. The mafic-ultramafic intrusions in the Dananhu arc have similar emplacement age and geochemical characteristics to those in Kangur shear belt and Middle Tianshan block, together with the denudation is relatively weak, which indicates that the Dananhu arc is an essential prospecting target for Cu-Ni mineralization in East Tianshan.

Keywords: magma source; sulfur saturation mechanism; isotopic characteristics; Yueyawan Cu-Ni deposit; East Tianshan

新疆东天山地区是世界上造山带型铜镍硫化物成矿作用最强烈的地区(宋谢炎等, 2018, 2022; 高晓峰等, 2025),产出有黄山、黄山东和图拉尔根等大型矿床,以及香山、葫芦、土墩、天宇和白石泉等一系列中小型矿床(李彤泰, 2011; 尹希文, 2015; 刘隆等, 2025),镍总储量达到百余万 t,是中国第二大镍资源基地(Qin et al., 2003; 刘德权等, 2005; 王京彬等, 2006; 张照伟等, 2021)。这些矿床均形成于早二叠世,延深大断裂成群成带分布,主要发育在康古尔韧性剪切带和中天山地块内(Zhou et al., 2004; Mao et al., 2008; Qin et al., 2011; Deng et al., 2014, 2020; Zhao et al., 2022; 石煜等, 2022)。近年来,在康古尔断裂以北的大南湖岛弧带不断取得找矿突破,发现了白鑫滩、路北和月牙湾等中小型铜镍矿床以及三宫、沙山、大草滩等矿化岩体(王亚磊等, 2016; Sun et al., 2019; 吕晓强等, 2020; Zhou et al., 2021, 2024),表明大南湖岛弧带具有优越的铜镍硫化物矿床找矿潜力。

前人对东天山铜镍成矿带中的赋矿岩体开展了大量的年代学和地球化学研究,取得了丰硕的研究成果。但是对于成矿岩浆活动的构造背景认识分歧较大,马瑞士等(1997)、白云来(2000)认为这些岩体是蛇绿岩套的组成部分;刘德权等(1992)、Xiao 等(2004)认为这些岩体是阿拉斯加型镁铁–超镁铁质岩体;一些学者认为是后碰撞阶段地壳伸展作用形成(韩宝福等, 2004; 王京彬等, 2006; Wang et al., 2008; 邓宇峰等, 2011; Gao et al., 2013);Zhou 等(2004)、Pirajno 等(2008)认为是地幔柱成因;也有部分学者认为是后碰撞伸展作用和地幔柱叠加(Qin et al., 2011; Su et al., 2011)。另一方面,硫化物的饱和机制也存在很大争议,壳源硫的加入可能导致了黄山东、黄山、葫芦等矿床中硫化物的饱和(Tang et al., 2013; Deng et al., 2015; Mao et al., 2016),但 Deng 等(2022)认为围岩地层中的硫并未被混染,地壳硫的混染过程发生在深部岩浆房。

月牙湾铜镍硫化物矿床位于大南湖岛弧带北缘,远离康古尔深大断裂,为以上争议问题的解决提供了新的窗口。笔者以月牙湾岩体为研究对象,开展了岩体地质,岩石 Sr、Nd、Pb 和硫化物原位 S 同位素研究,以期查明月牙湾岩体的岩浆源区和硫饱和机制,并探讨了大南湖岛弧带的铜镍成矿潜力。

1 区域地质背景

中亚造山带位于西伯利亚克拉通和塔里木-华北克拉通之间,由大陆微地块、岛弧和大洋地壳混杂拼合构成(Jahn et al., 2000; Xiao et al., 2013)。天山造山带位于中亚造山带南缘,在长期的演化过程中经历了极其复杂的裂解与拼合,由北向南可划分为北天山、中天山和南天山(Windley et al., 1990; 秦克章等, 2012; Xiao et al., 2013)。东天山包括北天山和中天山东段(Xiao et al., 2004; 韩春明等, 2018),自北向南依次划分为哈尔里克岛弧带、吐哈盆地、觉罗塔格构造带和中天山地块,其中觉罗塔格构造带由北向南可以划分为大南湖岛弧、康古尔剪切带和雅满苏弧后盆地(图 1)(Xiao et al., 2004)。区域地层出露比较齐全,以

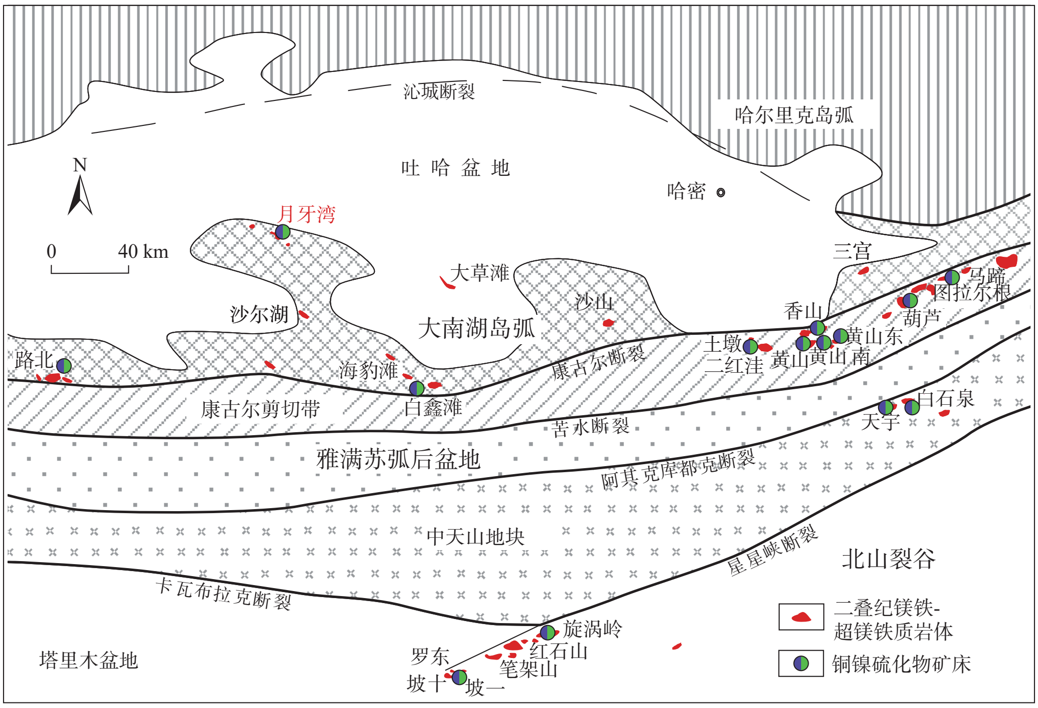

图1　东天山构造格架及二叠纪镁铁–超镁铁质岩体分布图(据秦克章等，2012 修)

Fig. 1　Map of the tectonic framework and Permian mafic-ultramfic intrusions in East Tianshan

康古尔深大断裂为界, 以北出露大柳沟组、大南湖组和头苏泉组的一套钙碱性岛弧火山岩和内碎屑岩建造; 以南出露梧桐窝子组、干墩组和雅满苏组的一套滨浅海相火山–沉积岩系建造组合, 中天山地块内发育前寒武系陆源碎屑岩的变质岩相(刘德权等, 1992)。区域断裂构造主要呈 EW 向展布, 沿康古尔断裂和阿奇克库都克断裂发育上百个镁铁–超镁铁质小岩体, 并发育多个铜镍硫化物矿床, 形成了黄山–镜儿泉矿集区和白石泉–天宇矿集区(王玉往等, 2009; 秦克章等, 2012; 三金柱, 2012; Deng et al., 2015; Mao et al., 2016; Shi et al., 2018; Deng et al., 2022; 石煜等, 2022)。在大南湖岛弧带形成了白鑫滩、路北和月牙湾铜镍矿床(Feng et al., 2018; 赵冰冰等, 2018; 周国超等, 2019; Zhou et al., 2021)。

2　矿床地质特征

月牙湾铜镍矿床位于卡拉塔格古生代隆起的中西部, 岩体侵入到下泥盆统大南湖组中基性火山岩–火山碎屑岩建造之中(图 2a)。月牙湾岩体平面上形似新月状, 南部为 NS 向延伸, 北部转为 NW 展布, 向 NW 拖尾(图 2b)。沿走向总体长约为 1.2 km, 宽约为 200～500 m, 面积约为 0.53 km^2。剖面上横截面呈“V”字形(图 2c), 纵剖面上呈一向北倾伏的岩管状, 南端抬起, 北部较深。月牙湾矿床的矿体主要受岩相带构造控制, 呈脉状和透镜状, 具有明显的“岩体底部控矿”的特征(图 2d)。Cu 品位为 0.20%～0.87%, 最高为 4.83 %, Ni 品位为 0.20%～0.36%, 最高为 1.76 %, 总体显示 Cu>Ni 的地质特征。

岩石类型由北向南及由浅到深显示规律性的分布。在地表由南向北岩石色率逐渐降低, 矿物粒度逐渐增大, 岩石基性程度逐渐降低, 岩性依次发育有橄榄辉长岩、细粒橄长岩、粗粒橄长岩和淡色辉长岩(图 2b)。在剖面上, 由浅到深, 岩石色率增高, 矿物粒度变细, 岩石基性程度增高, 主要岩性有辉长岩、橄长岩、橄榄辉长岩、暗色细粒橄榄辉长岩和暗色细粒橄长岩(图 2c)。

各岩相野外穿插关系表明月牙湾岩体是多期次岩浆侵位形成的复式岩体(Zhou et al., 2021)。第一期岩浆作用形成淡色辉长岩、辉长岩、橄长岩和橄榄辉长岩, 彼此之间过渡接触, 矿物组成基本一致、含量略有差别, 基性斜长石含量＞60%, 橄长岩中单斜辉石含量为＜10%(图 3a), 而橄榄辉长岩中单斜辉石(＞20%)常包裹橄榄石发育(图 3b)。第二期岩浆作用形成暗色细粒橄榄辉长岩和暗色细粒橄长岩, 是主要的赋矿岩相, 发育在岩体的下部层位。橄榄石含量 30%～

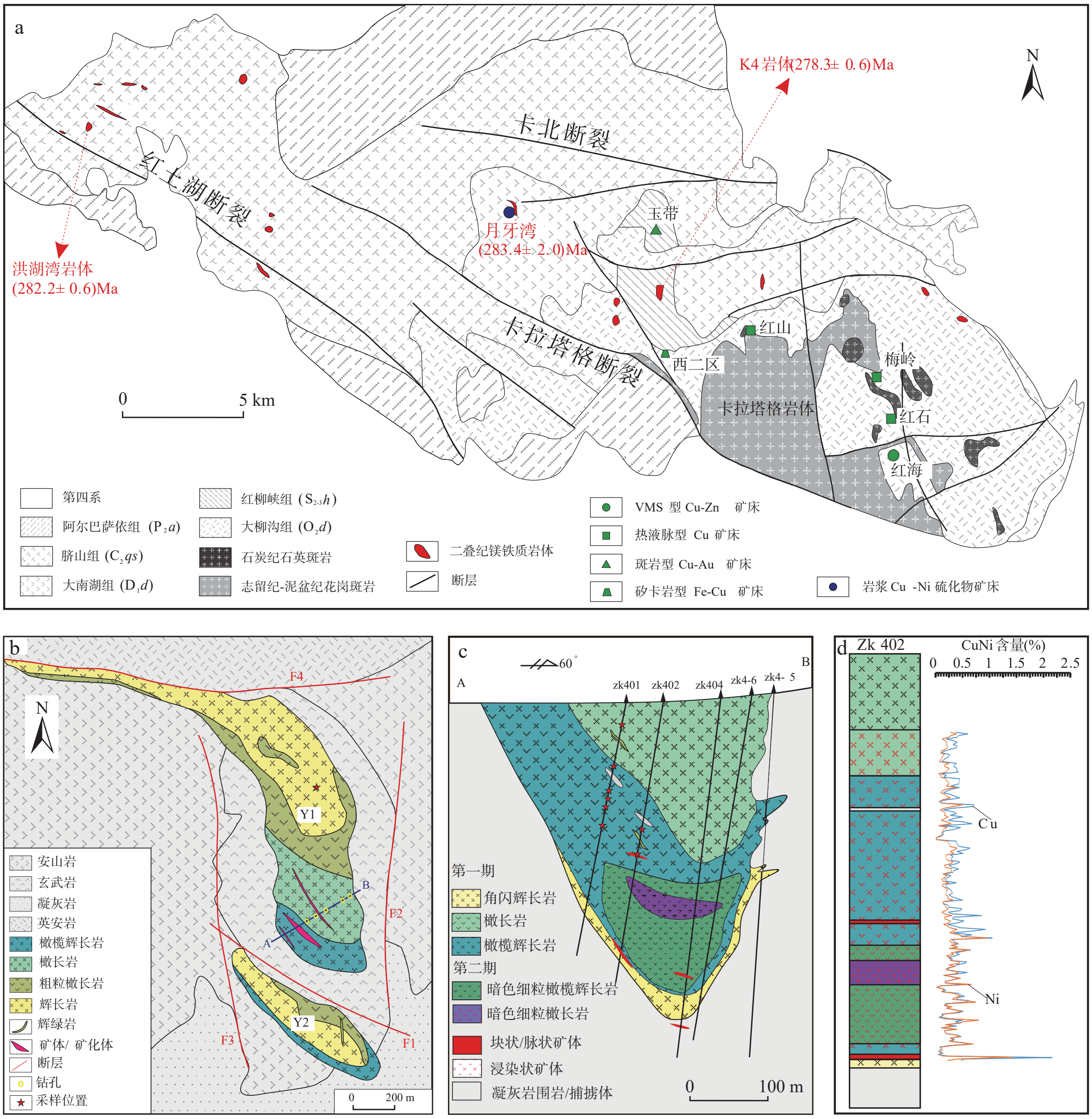

图2 卡拉塔格地质图(a)(据 Deng et al., 2016 修)、月牙湾岩体地质图(b)、剖面图(c)和 ZK402 柱状图(d)(据 Zhou et al., 2021 修)

Fig. 2 (a) Geological map of the Karatag area, (b) geological map, (c) cross-section, and (d) ZK402 borehole diagram of Yueyawan intrusion

60%, 基性斜长石含量＜30%, 发育一定量角闪石(～10%)。暗色细粒橄榄辉长岩发育含长嵌晶结构和包橄结构(图 3c), 含硫化物(5%～15%)。暗色细粒橄长岩基性斜长石呈细粒自形(图 3d), 含量为 10%～20%, 硫化物含量最高(10%～30%)。

3 采样及分析方法

本次研究中岩石样品采自地表露头(图 2b), 矿石样品采自勘探钻孔(图 2c)。岩矿石样品新鲜、有代表性。

Sr-Nd-Pb 同位素分析在中国科学院地质与地球物理研究所完成。Pb 同位素测试采用美国 Thermofisher 公司 Triton Plus 型热电离质谱仪。将纯化好的样品用微量盐酸溶解, 并加 1 微升硅胶和磷酸混合发射剂于铼灯丝表面, 质谱测量温度为 1 250 ± 50 ℃。国际标样 NIST981 被用于监控质谱仪状态。Sr-Nd-Pb 同位素测试采用 Thermofisher Triton Plus 多接收热

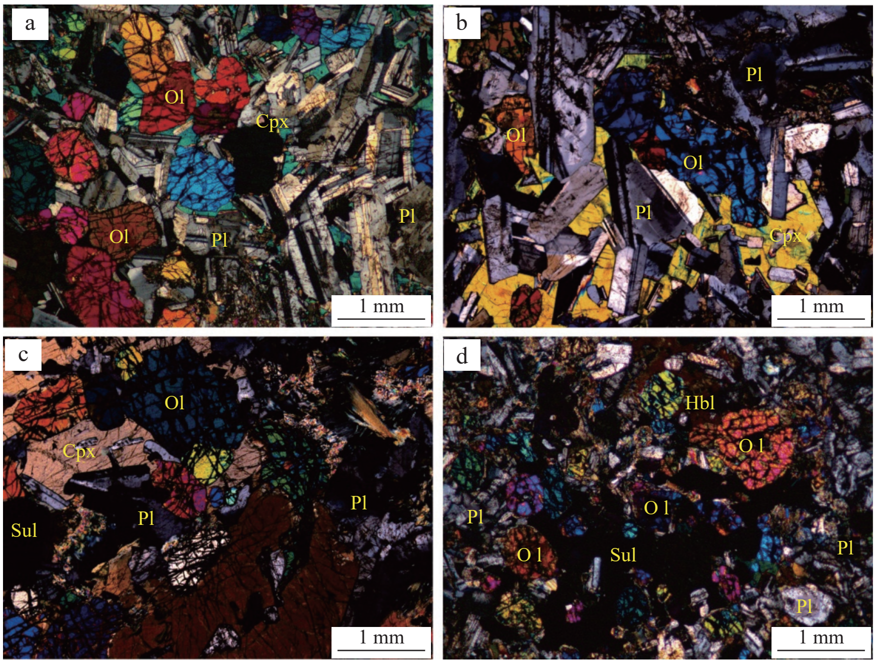

a. 橄长岩；b. 橄榄辉长岩；c. 暗色细粒橄榄辉长岩；d. 暗色细粒橄长岩；Ol. 橄榄石；Pl. 斜长石；Cpx. 单斜辉石；Hbl. 角闪石；Sul. 硫化物

图3　月牙湾岩体不同岩石显微照片

Fig. 3　Photomicrographs in cross-polarized light showing the dominant textures of the typical rocks.

电离质谱仪，全流程本底 Sr 和 Nd 分别小于 250 pg 和 100 pg，用 $^{88}Sr/^{86}Sr=8.375\,209$ 和 $^{146}Nd/^{144}Nd=0.721\,9$ 对 Sr 和 Nd 同位素比值进行校正，铅流程本底小于 200 pg，Pb 同位素质量分馏校正系数为每质量单位 1.2‰。用国际标样 NBS-987 和 JNdi-1 对仪器稳定性进行监测。详细的分析方法见 Li 等(2012, 2015)。

激光剥蚀多接收杯电感耦合等离子体质谱(LA-MC-ICP-MS)硫化物原位 S 同位素测试在北京锆年领航科技有限公司完成。质谱仪型号(MC-ICP-MS)型号为 Nu Plasma Ⅱ，激光器型号为 RESOlution-S155 193 nm ArF 准分子激光器。激光剥蚀系统使用氦气作为载气，同时辅以氩气混合少量氮气。样品测试激光束斑直径为 33 μm，剥蚀频率为 10 Hz，激光能量密度为 3. 0～4. 0 J/cm。测试 $\delta^{34}S$ 精度小于 0.1%。

4　分析测试结果

月牙湾岩体 Sr-Nd-Pb 同位素组成见表 1。$(^{87}Sr/^{86}Sr)_i$ 和 $\varepsilon_{Nd}(t)$ 根据橄长岩锆石 U-Pb 年龄 t=283.4 Ma 计算 (Zhou et al., 2021)。Sr-Nd 同位素变化范围较窄，具有低 $(^{87}Sr/^{86}Sr)_i$ 和高 $\varepsilon_{Nd}(t)$ 的特征，岩体 $(^{87}Sr/^{86}Sr)_i$ 变化范围分别为 0.703 3～0.703 48，平均值为 0.703 38，略高于洋中脊玄武岩(MORB, 0.702 29～0.703 16)(Saunders et al., 1992)，位于以夏威夷火山岩为代表的洋岛玄武岩(OIB)范围之内(0.703 17～0.704 12)Still et al., 1983)。岩体 $\varepsilon_{Nd}(t)$ 为 6.54～8.35，平均值为 7.73。月牙湾岩体 Pb 同位素比值较低，变化也较小，$(^{206}Pb/^{204}Pb)_i$=17.828～18.014，$(^{207}Pb/^{204}Pb)_i$=15.446～15.478，$(^{208}Pb/^{204}Pb)_i$=37.495～37.698。

月牙湾矿石中硫化物原位 S 同位素测试结果见表 2。磁黄铁矿、镍黄铁矿和黄铜矿 $\delta^{34}S$ 值分别为 2.01‰～4.09‰，0.03‰～2.12‰和 1.65‰～2.30‰，变化范围较窄。

5　讨论

5.1　岩浆源区

随着更多镁铁–超镁铁质岩体的岩相研究和更加精确的年代学测定，越来越多的地质学和年代学证据表明东天山地区二叠纪镁铁–超镁铁质岩体是幔源岩浆热侵位方式形成的，与蛇绿岩套无关(赵云等, 2016; 周国超等, 2019)。岩体的形成年龄明显晚于东天山区域俯冲碰撞事件结束时间(～300 Ma, Zhou et al., 2004; Qin et al., 2011; Su et al., 2011)，岩体形态也未见

表 1　月牙湾岩体 Sr, Nd, Pb 同位素数据表

Tab. 1　Sr, Nd, Pb isotope data of the Yueyawan intrusion

岩石名称	辉长岩	橄长岩		橄榄辉长岩		
样号	YYW7710-7	Y401-1	Y401-6	Y401-13	Y401-14	Y401-20
Rb (10^{-6})	2.95	2.28	2.9	1.62	2.29	1.49
Sr (10^{-6})	771	475	487	319	437	520
$^{87}Rb/^{86}Sr$	0.011 08	0.013 90	0.017 24	0.014 70	0.015 17	0.008 30
$^{87}Sr/^{86}Sr$	0.703 46	0.703 429	0.703 412	0.703 537	0.703 428	0.703 336
($^{87}Sr/^{86}Sr$) i	0.703 42	0.703 37	0.703 34	0.703 48	0.703 37	0.703 3
Nd (10^{-6})	6.9	7.57	9.18	2.68	8.83	6.89
Sm (10^{-6})	1.71	1.89	2.49	0.622	2.25	1.67
$^{147}Sm/^{144}Nd$	0.149 83	0.150 94	0.163 98	0.140 31	0.154 05	0.146 53
$^{143}Nd/^{144}Nd$	0.512 944	0.512 962	0.512 985	0.512 869	0.512 987	0.512 951
($^{143}Nd/^{144}Nd$) i	0.512 668	0.512 684	0.512 683	0.512 611	0.512 704	0.512 682
εNd(t)	7.65	7.96	7.94	6.54	8.35	7.92
Th (10^{-6})	0.29	0.18	0.19	0.15	0.20	0.23
U (10^{-6})	0.05	0.07	0.07	0.08	0.08	0.09
Pb (10^{-6})	11.2	4.17	4.03	4.23	1.37	2.37
($^{206}Pb/^{204}Pb$) i	18.013 5	17.932 1	17.859 3	17.827 8	17.843 8	17.855 1
($^{207}Pb/^{204}Pb$) i	15.478 0	15.465 9	15.462 3	15.455 7	15.446 0	15.454 7
($^{208}Pb/^{204}Pb$) i	37.698 3	37.614 9	37.554 3	37.523 1	37.494 7	37.521 9

注：Rb、Sr、Sm、Nd同位素计算参数：$\lambda(Sr)=1.42\times10^{-11}\ a^{-1}$，$\lambda(Nd)=0.654\times10^{-11}\ a^{-1}$，$(^{87}Sr/^{86}Sr)_{CHUR}=0.704\,5$，$(^{143}Nd/^{144}Nd)_{CHUR}=0.512\,638$; Pb初始同位素计算参数：$\lambda_1=1.551\,25\times10^{-11}\ a^{-1}$，$\lambda_2=9.848\,5\times10^{-11}\ a^{-1}$，$\lambda_3=0.494\,75\times10^{-11}\ a^{-1}$，t=283.4 Ma。

表 2　月牙湾矿床矿石硫化物 S 同位素组成

Tab. 2　S isotope compositions of the sulfides in Yueyawan intrusion

序号	样品号	测试矿物	$\delta^{34}S$(VCDT)
1	402-24-1po-1	磁黄铁矿	2.82
2	402-24-2po-1	磁黄铁矿	2.73
3	402-24-3-po-1	磁黄铁矿	2.01
4	402-24-3pn-1	镍黄铁矿	2.12
5	402-40-3pn-1	镍黄铁矿	0.03
6	y1-10-2po-1	磁黄铁矿	4.09
7	402-40-2cp-1	黄铜矿	2.30
8	402-24-2cp-1	黄铜矿	1.65

典型的环状结构。因此，与附冲背景下的阿拉斯加型岩体也不相同(Mao et al., 2008; Han et al., 2010; Gao et al., 2013)。越来越多的研究认为东天山二叠纪镁铁–超超镁铁质岩体形成于碰撞后伸展环境(Zhou et al., 2004; 顾连兴等, 2006; Wang et al., 2008; 王玉往等, 2009; 唐冬梅等, 2009; Song et al., 2011; 邓宇峰等, 2011, 2012)，争议主要在于其是否与塔里木地幔柱有关(夏林圻等, 2006; Mao et al., 2008; Pirajno et al., 2008; Qin et al., 2011)。

虽然有研究认为地幔柱作用形成大火成岩省可持续 15 Ma(Griffiths et al., 1990)，但东天山地区的镁铁–超镁铁质岩体形成的时间跨度显然更长(269～300 Ma)。再者，东天山地区未发现同期大规模溢流玄武岩以及地壳抬升，岩石中大量含水矿物的存在等特征都与典型地幔柱岩浆作用不同。薛胜超(2016)研究认为地幔柱作用下幔源岩浆在地壳上的就位会随着时间的变化而改变其最终就位位置，但是北山–天山地区时间跨度达 25 Ma 的二叠纪镁铁–超镁铁岩体，并没有表现出地幔柱成因模式下玄武质岩浆活动产物在时间和空间上的有序组合。

月牙湾岩体的($^{87}Sr/^{86}Sr$)$_i$、$\varepsilon_{Nd}(t)$和($^{206}Pb/^{204}Pb$)$_i$同位素组成与二叠纪塔里木大火成岩省玄武岩和镁铁-超镁铁质岩体均存在明显不同(图 4)。在($^{87}Sr/^{86}Sr$)$_i$-$\varepsilon_{Nd}(t)$图解上(图 4a)，月牙湾岩体的样品均位于第二象限，显示亏损地幔特征，且具有 MORB 相似的 Sr-Nd-Pb 同位素组成(图 4b～图 4d)。另一方面，包括月牙湾岩体在内的东天山地区二叠纪镁铁–超镁铁质岩石微量元素都显示不同程度的亏损 Nb、Ta、Ti 等高场强元素，相关岩石构造图解也表明岩石具有岛弧玄武岩和 MORB 共同的特征，而与吐哈玄武岩和塔里木玄武岩所处的板内玄武岩区域明显不同(图 5)。微量元素 Nb、Ta、Ti 的亏损表明岩浆源区混合了富集地幔

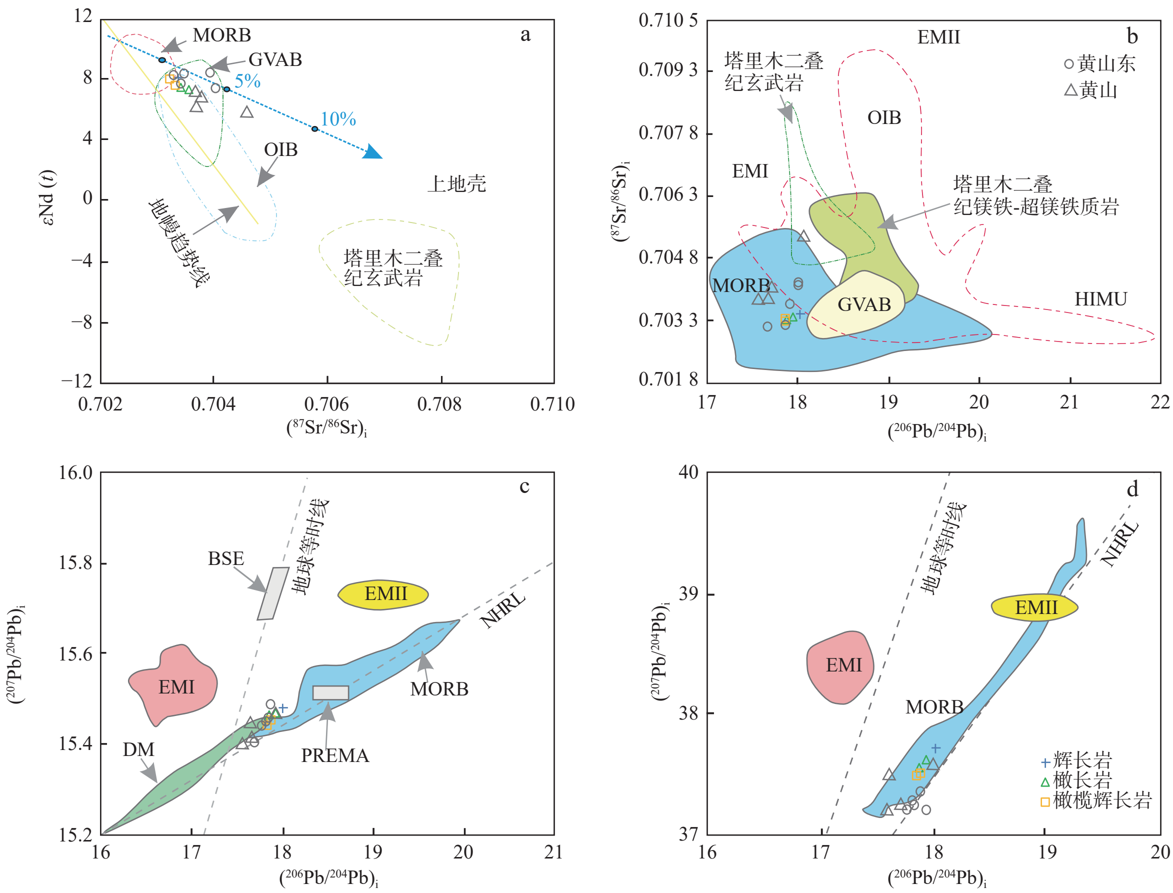

黄山东数据引自 Sun 等(2013); 黄山数据引自夏明哲(2009); 全球岛弧玄武岩(GVAB)数据引自 http://www.petdb.Org; 塔里木镁铁–超镁铁质岩数据引自 Zhou 等(2009); 塔里木玄武岩数据引自 Yuan 等(2012); DM. 亏损地幔; OIB. 洋岛玄武岩; MORB. 洋中脊玄武岩; PREMA. 原始地幔; BES. 大硅质地球; HIMU. 高 U/Pb 值地幔; EMI. I 型富集地幔; EMII. II 型富集地幔

图4　月牙湾岩体及有关岩石的 Sr-Nd-Pb 同位素图解

Fig. 4　Plots of Sr-Nd-Pb isotopes for the mafic rocks in Yueyawan intrusion

组分, 可能是岩浆源区遭受了俯冲事件的改造(邓宇峰等, 2011; Song et al., 2011; Zhao et al., 2016; 周国超等, 2019)。Nb-Nb/U 图解显示月牙湾等东天山镁铁–超镁铁质岩石微量处于弧火山岩和和洋中脊玄武之间(图 6a), La/Nb-La/Ba 图解显示地幔源区以俯冲交代的岩石圈地幔为主, 也有软流圈地幔的加入(图 6b)。因此, 包括月牙湾岩体在内的东天山地区二叠纪镁铁–超镁铁质岩形成于后碰撞伸展环境, 岩石地球化学既表现 MORB 的性质, 也表现弧火山岩的性质, 说明岩浆作用虽然发生在伸展背景之下, 但受到俯冲物质的显著交代。

5.2　S 饱和机制

幔源岩浆侵入到地壳后, 岩浆中硫达到饱和发生熔离是形成岩浆铜镍硫化物矿床的关键步骤(Barnes et al., 2005; Naldrett, 2010)。大量实验研究发现基性岩浆中硫的溶解度主要受控于岩浆的温度、压力、化学组分、氧逸度和硫逸度等因素(Haughton et al, 1974; Wendlandt, 1982; Mavrogenes et al., 1999; Li et al., 2005; Liu et al., 2007; Wykes et al., 2015)。导致岩浆硫达到饱和的机制主要有(Barnes et al., 2005; Li et al., 2005; Naldrett, 2010): ①地壳混染。②岩浆的结晶分异。③岩浆混合。④岩浆快速降温。⑤压力增大。其中对硫饱和最关键也最受争议的是壳源 S 是否加入。壳源 S 的混染被认为在很多超大型矿床成矿过程中扮演了重要角色。Noril'sk 矿床混染了围岩中的膏岩层(Li et al., 2003), Voisey's Bay 矿床混染了副变质片麻岩中的硫(Li et al., 2001), Duluth、金川、夏日哈木和黄山东等矿床的 $\delta^{34}S$ 值均被认为混染了围岩硫(Ripley et al., 2013; Deng et al., 2016; Liu et al., 2018)。

月牙湾矿床硫化物原位 $\delta^{34}S$ 为 0.03‰～4.09‰,

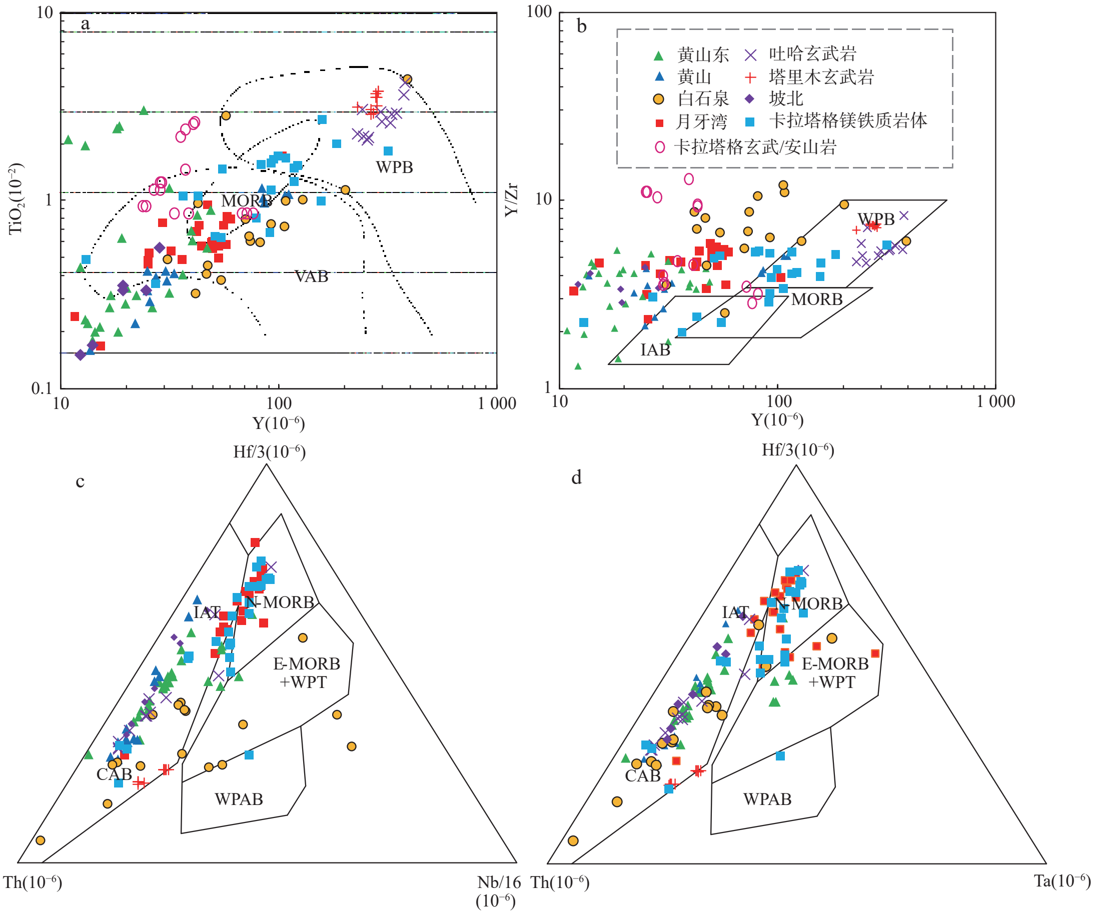

a、b 据 Pearce 等(1979)，WPB.板内玄武岩；MORB.洋中脊玄武岩；VAB.火山弧玄武岩；IAB.岛弧玄武岩；c、d 据 Wood(1990)，N-MORB.正常洋中脊玄武岩；E-MORB.富集洋中脊玄武岩；CAB.岛弧碱性玄武岩；IAT.岛弧拉斑玄武岩。数据来源：黄山东据夏明哲等(2010 和 Deng 等(2014)；黄山据 Deng 等(2015)；白石泉据毛启贵等(2006)和 Cha 等(2008)；月牙湾据 Zhou 等(2021)；坡北据颉炜等(2011)；吐哈玄武岩据唐冬梅等(2017)；塔里木玄武岩据 Yuan 等(2012)；卡拉塔格镁铁质岩体据周国超等(2019)；卡拉塔格安山/玄武岩据 Mao 等(2019)

图5 东天山二叠纪镁铁–超镁铁质岩石构造判别图解

Fig. 5 Tectonic environmental diagrams of Permian mafic-ultramafic intrusions in East Tianshan

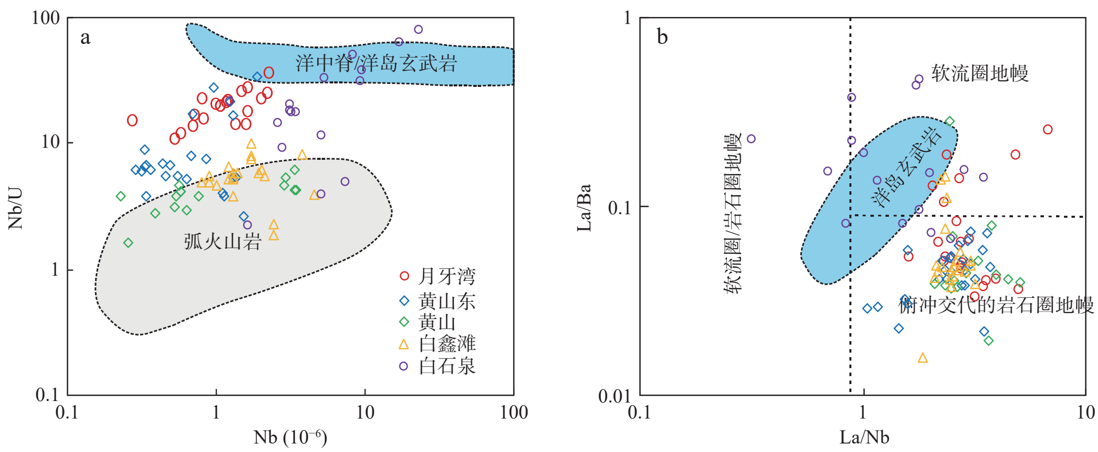

数据来源：黄山东据夏明哲等(2010)、Deng 等(2014)；黄山据 Deng 等(2015)；白石泉据毛启贵等(2006)、Chai 等(2008)；月牙湾据 Zhou 等(2021)；白鑫滩据王亚磊等(2015)

图6 东天山二叠纪镁铁–超镁铁质岩石 Nb-Nb/U（a）(据 Chung et al., 2001)和 La/Nb-La/Ba（b）(据 Fitton et al., 1991)图解

Fig. 6 (a) Nb-Nb/U and (b) La/Nb-La/Ba plots of Permian mafic-ultramafic intrusions in East Tianshan

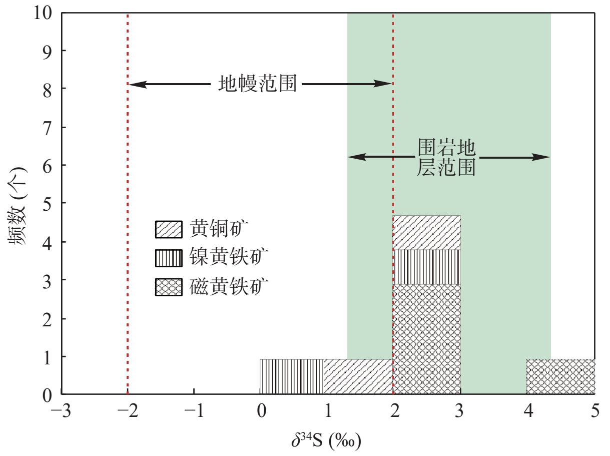

图7　东天山月牙湾铜镍硫化物矿石 S 同位素分布直方图

Fig. 7　S[34]δ frequency chart of sulfides in the Yueyawan deposit

大部分数据＞2‰, 位于地壳 $\delta^{34}S$ 范围之内(图 7), 而且与卡拉塔格地区石炭纪—二叠纪围岩地层 $\delta^{34}S$ 范围(1.4‰～4.4‰)(于明杰, 2016)一致, 表明月牙湾矿床成矿过程中混染了围岩地层中的 S。Se 属亲铜元素, 通常在地壳岩石中含量低, 而在幔源岩石中含量较高, 幔源岩石 Se/S 值高(230×10^{-6}～350×10^{-6}), 而地壳岩石 Se/S 值较低(＜50×10^{-6})。因此, Se/S 值可作为一个衡量壳源硫混入的重要地球化学指示剂(Eckstrand et al., 1989; Mc Donough et al., 1995)。月牙湾矿石样品 Se/S 值为 125×10^{-6}～332×10^{-6}(Zhou et al., 2021), 表明有壳源硫的加入。吕晓强等(2020)测定月牙湾矿石硫化物 $^{187}Os/^{188}Os$ 初始值为 0.279 6±0.008 9, 远大于原始地幔 $^{187}Os/^{188}Os$ 初始值(0.11～0.15), γOs 值为 117～126, 指示在成矿过程中有地壳物质的显著加入(Taylor et al., 1985)。

5.3　大南湖岛弧带铜镍成矿潜力

卡拉塔格地区发育包括月牙湾岩体在内的多个二叠纪镁铁–超镁铁质岩体, 其岩体特征、成岩时代和地区化学特征与康古尔剪切带和中天山地块等不同构造单元内成矿的镁铁–超镁铁质岩相似(表 3), 表明它们具有相似的地幔源区和岩浆演化过程。与

表 3　东天山二叠纪铜镍硫化物矿床特征表

Tab. 3　Main features of the major Cu-Ni sulfide deposits in the Eastern Tianshan

矿床	岩体面积(km²)	岩体形态	赋矿岩石组合	成矿年龄(Ma)	岩石 SiO_2 含量(%)	岩石 $Mg^{\#}$(%)	微量元素	$\delta^{34}S$(‰)	$\varepsilon Nd(t)$	参考文献
大南湖岛弧带										
月牙湾	0.53	新月状	橄榄辉长岩–橄长岩	283.4±2.0	33.04～50.26	43～83	富集Rb、Ba、Sr、K，亏损Th、Nb、Ta、Ti	0.03～4.09	6.54～8.35	本文; Sun et al., 2019; Zhou et al. 2021
白鑫滩	2.1	葫芦状	橄榄辉长岩–辉石橄榄岩	277.9±2.6	40.86～49.56	73～81	富集Rb, Th, U, La; 亏损Nb、Ta、Ti	−0.13～0.9	4.2～6.5	王亚磊等，2015; Feng et al., 2018; Deng et al., 2020
康古尔剪切带										
黄山	1.71	镰刀状	辉长岩–二辉橄榄岩	283.8±3.4	36.61～52.58	60～86	富集Rb、Ba、Sr; 亏损Nb、Ta、Ti	−1.8～0.86	5.83～7.46	邓宇峰等，2012; Deng et al., 2015
黄山东	2.8	菱形	二辉橄榄岩–橄榄辉长岩	282±20	36.1～50.5	44～77	富集Rb、Ba、Th、U相; 亏损Nb、Ta、Ti	−0.79～2.78	6.6～10.5	夏明哲等，2009; 邓宇峰等，2011; Deng et al., 2014
图拉尔根	＜0.01	脉状	二辉岩–二辉橄榄岩	300.5±3.2	24.36～47.8	51～83	富集Rb, Ba、Th; 亏损Nb, Ta	−1.3～3.8	3.22～7.17	焦建刚等，2012; Xue et al., 2022
葫芦	0.75	葫芦形	橄榄岩–辉石岩–辉橄岩	283±13	29.67～56.14	42～87	富集Th、U; 亏损Nb、Ta、Ti	1.46～4.87	6.5～7.1	Han et al., 2013; Zhao et al., 2016
香山西	1.6	菱形	辉长岩–辉石岩–橄榄岩	283±3	39.3～53.4	38～81	富集Th、U; 亏损Nb、Ta、Ti	−0.84～2.4	5.9～6.7	Han et al., 2010; Shi et al., 2018
土墩	0.8	椭圆形	二辉橄榄岩	298.4±0.9	37.02～48.96	26～84	富集K、Sr、Ba、U; 亏损Nb、Ta、Ti、P	−0.6～0.7		陈继平等，2016
中天山地块										
白石泉	0.8	不规则状	橄榄岩–橄榄辉石岩	284±8	37.89～51.52	41～83	富集La，U，Zr; 亏损Nb，Ta，Ti	1.4～5.4	1.67～7.61	Chai et al., 2008, 陈斌等，2013
天宇	0.056	脉状	橄榄岩–橄榄辉石岩	290.2±3.4	35.89～53.52	33～81	富集Rb、Ba、Th、U; 亏损Nb，Ta，Zr	5.1～8.2	−0.7～5.7	唐冬梅等，2009

康古尔剪切带和中天山地块不同的是，在卡拉塔格地区外围发育一定规模的二叠纪玄武质–安山质–流纹质火山岩（Mao et al., 2019）。这些同期火山岩与月牙湾岩体具有相似的 Sr-Nd 同位素体系，主量元素含量连续变化（图 8），说明这些同期火山岩可能是月牙湾岩体的岩浆系统的前导性岩浆形成的，而在中天山地块和康古尔剪切带中的同时期玄武岩可能是被剥蚀掉了（Mao et al., 2008），这说明大南湖岛弧带的剥蚀程度较浅，可能存在进一步找寻铜镍硫化物矿床的潜力。

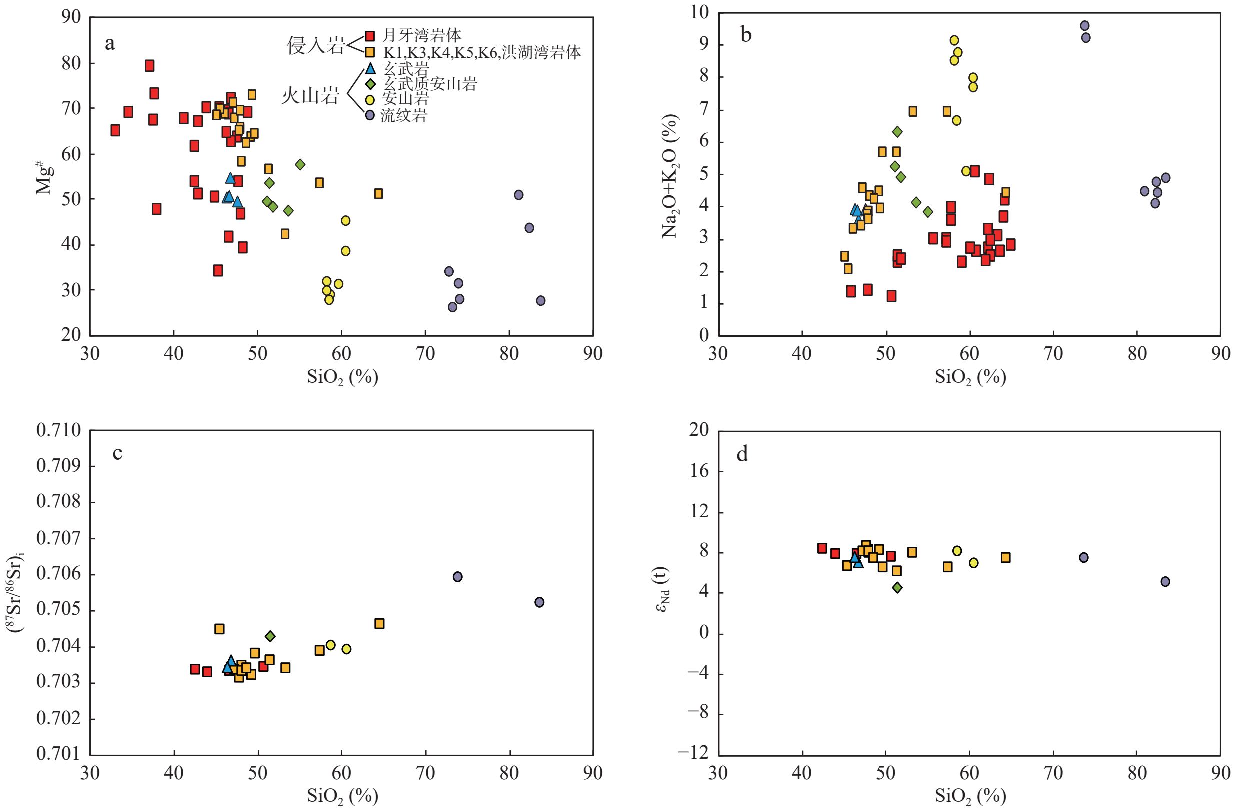

火山岩数据引自 Mao 等（2019）；K1-K6 和洪湖湾岩体数据引自周国超等（2019））；月牙湾岩体数据引自 Zhou 等（2021）

图8 卡拉塔格地区二叠纪岩石地球化学图解

Fig. 8 Geochemical diagrams of Permian rocks in Karatag area

最新勘查工作表明，除月牙湾矿床外，卡拉塔格地区的 K4 岩体和洪湖湾岩体也发育铜镍矿化（周国超等, 2019）。在大南湖岛弧带西段，已经发现了路北和白鑫滩中小型矿床，向东有海豹滩、大草滩、沙山和三宫的镁铁–超镁铁质岩体，成岩年龄均为早二叠世，且发育不同程度的铜镍矿化（王亚磊等, 2015; Feng et al., 2018）。因此，笔者认为在勘查程度较弱的大南湖岛弧带具有较好的铜镍成矿潜力，是东天山地区铜镍找矿勘查的重点方向。

6 结论

（1）月牙湾岩体同位素与岩石地球化学既表现 MORB 的性质，也表现弧火山岩的性质，说明岩浆作用虽然发生在后碰撞伸展环境，但遭受了俯冲物质的显著交代。

（2）月牙湾铜镍硫化物矿床成矿过程中硫饱和及硫化物熔离可能主要与壳源硫的加入有关。

（3）大南湖岛弧带剥蚀程度较浅，勘查程度较弱，具有较好的铜镍成矿潜力。

致谢：本文野外工作得到哈密红石矿业公司王洋和张岩工程师的支持与协助；同位素分析得到了中国科学院地质与地球物理研究所李潮峰和李友连老师的指导；硫化物原位硫同位素测试得到了北京锆年领航科技有限责任公司章双荣老师的帮助；审稿人对本文提出了建设性的修改意见；在此致以诚

挚的谢意。

参考文献（References）：

白云来. 新疆哈密黄山—镜儿泉镍铜成矿系统的地质构造背景[J]. 甘肃地质学报，2000，2：1−7.

BAI Yunlai. Geotectonic setting of Huangshan-Jingerquan nikel-copper metallogenic system in Hami, Xinjiang[J]. Acta Geologica Gansu, 2000, 2: 1−7.

陈斌，贺敬博，陈长健，等. 东天山白石泉镁铁-超镁铁杂岩体的 Nd-Sr-Os 同位素成分及其对岩浆演化的意义[J]. 岩石学报，2013，29(1)：294−302.

CHEN Bin, HE Jingbo, CHEN Changjian, et al. Nd-Sr-Os isotopic data of the Baishiquan mafic-ultramafic complex from East Tianshan, and implications for petrogenesis[J]. Acta Petrologica Sinica, 2013, 29(1): 294−302.

陈继平，王晖，廖群安，等. 东天山土墩铜镍硫化物矿床成岩时代与岩石成因[J]. 地质科技情报，2016，35(6)：44−54.

CHEN Jiping, WANG Hui, LIAO Qunan, et al. Geochronological and Geochemical of Tudun Cu-Ni sulfide Deposits, East Tianshan[J]. Geological Science and Technology Infromation, 2016, 35(6): 44−54.

邓宇峰，宋谢炎，陈列锰，等. 东天山黄山西含铜镍矿镁铁-超镁铁岩体岩浆地幔源区特征研究[J]. 岩石学报，2011，27(12)：3640−3652.

DENG Yufeng, SONG Xieyan, CHEN Liemeng, et al. Features of the mantle source of the Huangshanxi Ni-Cu sulfide bearing mafic-ultramafic intrusion, eastern Tianshan[J]. Acta Petrologica Sinica, 2011, 27(12): 3640−3652.

邓宇峰，宋谢炎，周涛发，等. 新疆东天山黄山东岩体橄榄石成因意义探讨[J]. 岩石学报，2012，28(7)：2224−2234.

DENG Yufeng, SONG Xieyan, ZHOU Taofa, et al. Correlations between Fo number and Ni content of olivine of the Huangshandong intrusion, eastern Tianshan, Xinjiang, and the genetic significances[J]. Acta Petrologica Sinica, 2012, 28(7): 2224−2234.

高晓峰，隋清霖，尤敏鑫，等. 造山带岩浆铜镍硫化物矿床深部动力学机制探讨[J]. 西北地质，2025，58(3)：206−220.

GAO Xiaofeng, SUI Qinglin, YOU Minxin, et al. Study on Dynamic Mechanism of Magmatic Copper-Nickel Sulfide Deposits in Orogenic Belts[J]. Northwestern Geology, 2025, 58(3): 206−220.

顾连兴，张遵忠，吴昌志，等. 关于东天山花岗岩与陆壳垂向增生的若干认识[J]. 岩石学报，2006，22(5)：1103−1120.

GU Lianxing, ZHANG Zunzhong, WU Changzhi, et al. Some problems on granites and vertical growth of the continental crust in the eastern Tianshan Mountains, NW China[J]. Acta Petrologica Sinca, 2006, 22(5): 1103−1120.

韩宝福，季建清，宋彪，等. 新疆喀拉通克和黄山东含铜镍矿镁铁-超镁铁杂岩体的 SHRIMP 锆石 U-Pb 年龄及其地质意义[J]. 科学通报，2004，49(22)：2324−2328.

HAN Baofu, JI Jianqing, SONG Biao, et al. SHRIMP zircon U-Pb ages of Kalatongke No. 1 and Huangshandong Cu-Ni-bearing mafic-ultramafic complexes, North Xinjiang and geological implications[J]. Chinese Science Bulletin, 2004, 49(22): 2324−2328.

韩春明，肖文交，万博，等. 东天山晚古生代-中生代构造演化和内生金属矿床成矿系列[J]. 岩石学报，2018，34(7)：1914−1932.

HAN Chunming, XIAO Wenjiao, WAN Bo, et al. Late Palaeozoic-Mesozoic endogenetic tallogenic series and geodynamic evolution in the East Tianshan Mountains[J]. Acta Petrologica Sinica, 2018, 34(7): 1914−1932.

焦建刚，汤中立，钱壮志，等. 东天山地区图拉尔根铜镍硫化物矿床成因及成矿过程[J]. 岩石学报，2012，28(22)：3772−3786.

JIAO Jiangang, TANG Zhongli, QIAN Zhuangzhi, et al. Genesis and metallogenic process of Tulaergen large scale Cu-Ni sulfide deposit in eastern Tianshan area, Xinjiang[J]. Acta Petrologic Sinica, 2012, 28(22): 3772−3786.

刘德权，唐延龄，周汝洪. 中国新疆铜矿床和镍矿床 [M]. 北京：地质出版社，2005，1−306.

李彤泰. 新疆哈密市黄山基性-超基性岩带铜镍矿床地质特征及矿床成因[J]. 西北地质，2011，44(1)：54−60.

LI Tongtai. Geological Features and Metallogenesis of Cu-Ni Deposit in Basic-to-Ultrabasic Zone of Huangshan, Hami Area[J]. Northwestern Geology, 2011, 44(1): 54−60.

刘德权，唐延龄，周汝洪. 新疆北部古生代地壳演化与成矿系列[J]. 矿床地质，1992，11(4)：307−314.

LIU Dequan, TANG Yanling, ZHOU Ruhong. Evolution of Palaeozoic crust and metallogenic series in northern Xinjiang[J]. Mineral Deposits, 1992, 11(4): 307−314.

吕晓强，毛启贵，郭娜欣，等. 东天山卡拉塔格地区月牙湾铜镍硫化物矿床磁黄铁矿 Re-Os 同位素测定及其地质意义[J]. 地球科学，2020，45(9)：3475−3486.

LV Xiaoqiang, MAO Qigui, GUO Naxin, et al. Re-Os Isotopic Dating of Pyrrhotite from Yueyawan Cu-Ni Sulfide Deposit in Kalatage Area of East Tianshan Mountain and Its Geological Significance[J]. Earth Science, 2020, 45(9): 3475−3486.

刘隆，杜辉，唐小平，等. 东天山红石岗南地区隐伏地质体磁异常特征及其找矿指示[J]. 西北地质，2025，58(3)：97−107.

LIU Long, DU Hui, TANG Xiaoping, et al. Characteristics of Magnetic Anomalies and Geological Significance in the Southern Hongshigang Area of the Eastern Tianshan Mountains, China[J]. Northwestern Geology, 2025, 58(3): 97−107.

马瑞士，舒良树，孙家齐. 东天山构造演化与成矿 [M]. 北京：地质出版社，1997，1−202.

毛启贵，肖文交，韩春明，等. 新疆东天山白石泉铜镍矿床基性-超基性岩体锆石 U-Pb 同位素年龄、地球化学特征及其对古亚洲洋闭合时限的制约[J]. 岩石学报，2006，22(1)：153−162.

MAO Qigui, XIAO Wenjiao, HAN Chunming, et al. Zircon U-Pb age, geochemistry of the Baishiquan mafic-ultramafic complex in the eastern Tianshan, Xinjiang Province: Constraints on the closure of the Paleo-Asian Ocean[J]. Acta Petrologica Sinica, 2006, 22(1): 153−162.

秦克章, 唐冬梅, 苏本勋, 等. 北疆二叠纪镁铁-超镁铁岩铜、镍矿床的构造背景、岩体类型、基本特征、相对剥蚀程度、含矿性评价标志及成矿潜力分析[J]. 西北地质, 2012, 45(4): 83−116.

QIN Kezhang, TANG Dongmei, SU Benxun, et al. The Tectonic setting, style, basic feature, relative erosion degree, ore-bearing evaluation sign, potential analysis of mineralization of Cu-Ni-bearing Permian mafic-ultramafic complexes, northern Xinjiang[J]. Northwestern Geology, 2012, 45(4): 83−116.

三金柱. 黄山—镜儿泉铜镍矿带区域成矿规律探讨——以图拉尔根铜镍矿为例[J]. 西北地质, 2012, 45(4): 176−184.

SAN Jinzhu. An Approach to Regional Metallogenic Regularities of Cu-Ni Ore belt in Huangshan-Jingerquan in Xinjiang, China: A Case for Tulaergen Cu-Ni Deposits[J]. Northwestern Geology, 2012, 45(4): 176−184.

石煜, 王玉往, 王京彬, 等. 东天山黄山东和黄山西铜镍硫化物矿床含矿超镁铁岩的成岩–成矿作用机制: 来自斜长石成分的约束[J]. 地球科学, 2022, 47(9): 3244−3257.

SHI Yu, WANG Yuwang, WANG Jingbin, et al. Petrogenesis and Metallogenesis Mechanism of the Ore-Bearing Ultramafic Rocks from the Huangshandong and Huangshanxi Ni-Cu Sulfide Deposits, Eastern Tianshan: Constraints from Plagioclase Compositions[J]. Earth Science, 2022, 47(9): 3244−3257.

宋谢炎, 邓宇峰, 颉炜, 等. 新疆黄山-镜儿泉铜镍硫化物成矿带岩浆通道成矿特征及其找矿意义[J]. 矿床地质, 2022, 41(6): 1108−1123.

SONG Xieyan, DENG Yufeng, XIE Wei, et al. Ore-forming processes in magma plumbing systems and significances for prospecting of Huangshan-Jingerquan Ni-Cu sulfide metallogenetic belt, Xinajiang, NW China[J]. Mineral Deposits, 2022, 41(6): 1108−1123.

宋谢炎, 胡瑞忠, 陈列锰. 中国岩浆铜镍硫化物矿床地质特点及其启示[J]. 南京大学学报 (自然科学), 2018, 54(02): 221−235.

SONG Xieyan, HU Ruizhong, CHEN Liemeng. Characteristics and inspirations of the Ni-Cu sulfide deposits in China[J]. Journal of Nanjing University (Natural Science), 2018, 54(02): 221−235.

唐冬梅, 秦克章, 孙赫, 等. 天宇铜镍矿床的岩相学、锆石 U-Pb 年代学、地球化学特征: 对东疆镁铁-超镁铁质岩体源区和成因的制约[J]. 岩石学报, 2009, 25: 817−831.

TANG Dongmei, QIN Kezhang, SUN He, et al. Lithological chronological and geochemical characteristics of Tianyu Cu-Ni deposit, East Tianshan: Constraints on source and genesis of mafic-ultramafic intrusions in East Xinjiang[J]. Acta Petrologica Sinica, 2009, 25: 817−831.

唐冬梅, 秦克章, 薛胜超, 等. 吐哈盆地早二叠世玄武岩原始岩浆性质: 来自熔融包裹体成分的制约[J]. 岩石学报, 2017, 33(2): 339−353.

TANG Dongmei, QIN Kezhang, XUE Shengchao, et al. Nature of primitive magmas of Early Permian basalts in Tuha basin, Xinjiang: Constraints from melt inclusions[J]. Acta Petrologica Sinica, 2017, 33(2): 339−353.

王京彬, 徐新. 新疆北部后碰撞构造演化与成矿[J]. 地质学报, 2006, 80(1): 23−31.

WANG Jingbin, XU Xin. Post-collisional Tectonic Evolution and Metallogenesis in Northern Xinjiang, China[J]. Acta Geologica Sinica, 2006, 80(1): 23−31.

王亚磊, 张照伟, 尹希文, 等. 东天山三宫铜镍矿化岩体年代学、岩石地球化学特征及对 Cu-Ni 找矿的启示[J]. 地球学报, 2016, 37(6): 699−710.

WANG Yalei, ZHANG, Zhaowei, YIN Xiwen, et al. Chronological and geochemical characteristics of Sangong Cu-Ni mineralization intrusion in Eastern Tianshan of Xinjiang and their implications for Cu-Ni mineralization[J]. Acta Geosciences Sinica, 2016, 37(6): 699−710.

王亚磊, 张照伟, 尤敏鑫, 等. 东天山白鑫滩铜镍矿锆石 U-Pb 年代学、地球化学特征及对 Ni-Cu 找矿的启示[J]. 中国地质, 2015, 42(3): 452−467.

WANG Yalei, ZHANG Zhaowei, YOU Minxin, et al. Chronological and geochemical characteristics of the Baixintan Ni-Cu deposit in Eastern Tianshan Mountains, Xinjiang, and their implications for Ni-Cu mineralization[J]. Geology in China, 2015, 42(3): 452−467.

王玉往, 王京彬, 王莉娟, 等. 新疆香山铜镍钛铁矿区两个镁铁-超镁铁岩系列及特征[J]. 岩石学报, 2009, 25(4): 888−900.

WANG Yuwang, WANG Jingbin, WANG Lijuan, et al. Characteristics of two mafic-ultramafic rock series in the Xiangshan Cu-Ni-(V) Ti-Fe ore district, Xinjiang[J]. Acta Petrologica Sinica, 2009, 25(4): 888−900.

夏林圻, 李向民, 夏祖春, 等. 天山石炭-二叠纪大火成岩省裂谷火山作用与地幔柱[J]. 西北地质, 2006, 39(1): 1−49.

XIA Linqi, LI Xiangmin, XIA Zuchun, et al. Carboniferous-Permian rift-related volcanism and mantle plume in the Tianshan, Northwestern China[J]. Northwestern Geology, 2006, 39(1): 1−49.

夏明哲. 新疆东天山黄山岩带镁铁-超镁铁质岩石成因及成矿作用 [D]. 西安: 长安大学, 2009, 1−157.

XIA Mingzhe. The mafic-ultramafic intrusions in the Huangshangdong region, erstern Tianshan, Xinjiang: Petrogenesis and mineralization implication[D]. Xi'an: Chang'an University, 2009, 1−157.

夏明哲, 姜常义, 钱壮志, 等. 新疆东天山黄山东岩体岩石地球化学特征与岩石成因[J]. 岩石学报, 2010, 26(8): 2413−2430.

XIA Mingzhe, JIANG Changyi, QIAN Zhuagnzhi, et al. Geochemistry and petrogenesis of Huangshandong intrusion, East Tianshan, Xinjiang[J]. Acta Petrologica Sinica, 2010, 26(8): 2413−2430.

颉炜, 宋谢炎, 聂晓勇, 等. 新疆坡十铜镍硫化物含矿岩体岩浆源区特征及构造背景探讨[J]. 地学前缘, 2011, 18(3): 189−200.

XIE Wei, SONG Xieyan, NIE Xiaoyong, et al. Features of the mantle source and tectonic setting of the Poshi Ni-Cu sulfide-bearing intrusion, Xinjiang, China[J]. Earth Science Frontiers, 2011, 18(3): 189−200.

薛胜超. 新疆坡北二叠纪杂岩体岩浆过程、镍成矿作用及地球背景 [D]. 北京: 中国科学院大学, 2016.

XUE Shengchao. Magmatic process, nickel mineralization and geodynamic background of Permian Pobei mafic-ultramafic complex, Xinjiang[D]. Beijing: University of Chinese Academy of Sciences, 2016.

于明杰. 东天山卡拉塔格矿集区梅岭铜锌 (金) 矿床成矿作用 [D]. 北京: 中国地质大学 (北京), 2016.

YU Mingjie. Metallogeneses in relation to the Meiling Cu-Zn (Au) deposit in the Kalatage ore concentration area, Eastern Tianshan Mountain, Xinjiang, NW China[D]. Beijing: China University of Geosciences, 2016.

尹希文. 新疆香山铜镍硫化物矿床岩浆深部过程与找矿方向探讨[J]. 西北地质, 2015, 48(3): 22−30.

YIN Xiwen. Magma Deep Process and Prospecting Direction of Xiangshan Ni-Cu deposit, Eastern Tianshan, Xinjiang[J]. Northwestern Geology, 2015, 48(3): 22−30.

张照伟, 钱兵, 王亚磊, 等. 中国西北地区岩浆铜镍矿床地质特点与找矿潜力[J]. 西北地质, 2021, 54(1): 82−99.

ZHANG Zhaowei, QIAN Bing, WANG Yalei, et al. Geological Characteristics and Prospecting Potential of Magmatic Ni-Cu Sulfide Deposits in Northwest China[J]. Northwestern Geology, 2021, 54(1): 82−99.

赵冰冰, 邓宇峰, 周涛发, 等. 东天山白鑫滩含铜镍矿镁铁-超镁铁岩体的岩石成因: 年代学、岩石地球化学和 Sr-Nd 同位素证据[J]. 岩石学报, 2018, 34(9): 2733−2753.

ZHAO Bingbing, DENG Yufeng, ZHOU Taofa, et al. Petrogenesis of the Baixintan Ni-Cu sulfide-bearing mafic-ultramafic intrusion, East Tianshan: Evidence from geochronology, petrogeochemistry and Sr-Nd isotope[J]. Acta Petrologica Sinca, 2018, 34(9): 2733−2753.

赵云, 杨永强, 柯君君. 含铜镍岩浆起源及硫饱和机制: 以新疆黄山南岩浆铜镍硫化物矿床 Sr-Nd-Pb-S 同位素和元素地球化学研究为例[J]. 岩石学报, 2016, 32(7): 2086−2098.

ZHAO Yun, YANG Yongqiang, KE Junjun. Origin of Cu and Ni bearing magma and sulfide saturation mechanism: A case study of Sr-Nd-Pb-S isotopic composition and element geochemistry on the Huangshannan magmatic Ni-Cu sulfide deposit, Xinjiang[J]. Acta Petrologica Sinca, 2016, 32(7): 2086−2098.

周国超, 王玉往, 石煜, 等. 东天山卡拉塔格地区镁铁质岩体年代学、岩石地球化学研究[J]. 岩石学报, 2019, 35(10): 3189−3212.

ZHOU Guochao, WANG Yuwang, SHI Yu, et al. Geochronology and geochemistry of mafic intrusions in the Kalatag area, eastern Tianshan[J]. Acta Petrologica Sinica, 2019, 35(10): 3189−3212.

Barnes S J, Lightfoot P. The formation of magmatic nickel-coper-PGE sulfide deposits[J]. Economic Geology, 2005, 190: 135−154.

Chai Fengmei, Zhang Zhaochong, Mao Jingwen, et al. Geology, petrology and geochemistry of the Baishiquan Ni-Cu- bearing mafic-ultramafic intrusions in Xinjiang, NW China: Implications for tectonics and genesis of ores[J]. Journal of Asian Earth Sciences, 2008, 32: 218−235.

Chung Sunlin, Wang Kuolung, Crawford A J, et al. High-Mg potassic rocks from Taiwan: implications for the genesis of orogenic potassic lavas[J]. Lithos, 2001, 59: 153−170.

Deng Yufeng, Song Xieyan, Chen Liemeng, et al. Geochemistry of the Huangshandong Ni-Cu deposit in northwestern China: Implications for the formation of magmatic sulfide mineralization in orogenic belts[J]. Ore Geology Reviews, 2014, 56: 181−198.

Deng Yufeng, Song Xieyan, Hollings P, et al. Role of asthenosphere and lithosphere in the genesis of the Early Permian Huangshan mafic-ultramafic intrusion in the Northern Tianshan, NW China[J]. Lithos, 2015, 277: 241−254.

Deng Yufeng, Yuan Feng, Hollings P, et al. Magma generation and sulfide saturation of Permian mafic-ultramafic intrusions from the western part of the Northern Tianshan in NW China: implicaitons for Ni-Cu mineralization[J]. Mineralium Deposita, 2020, 55(7): 515−534.

Deng Yufeng, Song Xieyan, Xie Wei, et al. The Role of External Sulfur in Triggering Sulfide Immiscibility at Depth: Evidence from the Huangshan-Jingerquan Ni-Cu Metallogenic Belt, NW China[J]. Economic Geology, 2022, 117(8): 1867−1879.

Deng Xiaohua, Wang Jingbin, Pirajno F, et al. Re-Os dating of chalcopyrite from selected mineral deposits in the Kalatag district in the eastern Tianshan orogen, China[J]. Ore Geology Reviews, 2016, 77: 72−81.

Eckstrand O, Grinenko L, Krouse H, et al. Preliminary data on sulphur isotopes and Se/S ratios, and the source of sulphur in magmatic sulphides from the Fox River Sill, Molson Dykes and Thompson nickel deposits, northern Manitobal[J]. Current Research Part: C, Geological Survey of Canada, 1989, 89-1C, 235-242.

Feng Yanqing, Qian Zhuangzhi, Duan Jun, et al. Geochronological and geochemical study of the Baixintan magmatic Ni-Cu sulphide deposit: New implications for the exploration potential in the western part of the East Tianshan nickel belt (NW China)[J]. Ore Geology Reviews, 2018, 95: 366−381.

Fitton G J, James D, Leeman W P. Basic magmatism associated with late Cenozoic extension in the Western United States: Compositional variations in space and time[J]. Journal of Geophysical Research, 1991, 96(B8): 13693−13711.

Gao Jianfeng, Zhou Meifu, Lightfoot P C, et al. Sulfide Saturation and Magma Emplacement in the Formation of the Permian

Huangshandong Ni-Cu Sulfide Deposit, Xinjiang, Northwestern China[J]. Economic Geology, 2013, 108(8): 1833−1848.

Griffiths R W, Campbell I H. Stirring and structure in mantle starting plumes[J]. Earth and Planetary Letters, 1990, 99(1-2): 66−78.

Han Chunming, Xiao Wenjiao, Zhao Guochun, et al. In-situ U-Pb, Hf and Re-Os isotopic analyses of the Xiangshan Ni-Cu-Co deposit in eastern Tianshan (Xinjiang), Central Asia Orogenic Belt: Constraints on the timing and genesis of the mineralization[J]. Lithos, 2010, 120: 547−567.

Han Chunming, Xiao Wenjiao, Zhao Guochun, et al. SIMS U-Pb zircon dating and Re-Os isotopic analysis of the Hulu Cu-Ni deposit, eastern Tianshan, Central Asian Orogenic Belt, and its geological significance[J]. Journal of Geosciences, 2013, 58(3): 251−270.

Haughton D R, Roeder P L, Skeinner B J. Solubility of sulfur in mafic magmas[J]. Economic Geology, 1974, 69: 451−467.

Jahn BM, Wu Fuyuan, CHEN Bin. Granitoids of the Central Asian orogenic belt and continental growth in the Phanerozoic[J]. Royal Society of Edinburgh: Earth Science, 2000, 91: 181−193.

Li C, Naldrett A J, Ripley E M. Critical factors for the formation of a nickel-copper deposit in an evolved magma system: from a comparison of the Pants Lake and Voisey's Bay sulfide occurrences in Labrador, Canada[J]. Mineralium Deposita, 2001, 36(1): 86−92.

Li C, Ripley E M, Naldrett A J. Compositional variation of olivine and sulfur isotopes in the Noril'sk and Talnakh intrusions, Siberia: Implications for ore-forming processes in dynamic magma conduits[J]. Economic Geology, 2003, 98: 69−86.

Li C, Ripley E M. Empirical equations to predict the sulfur content of mafic magmas at sulfide saturation and applications to magmatic sulfide deposits[J]. Mineralium Deposita, 2005, 40, 218-230.

Li Chaofeng, Chu Z Y, Guo Jinghui, et al. A rapid single column separation scheme for highprecision Sr-Nd-Pb isotopic analysis in geological samples using thermal ionization mass spectrometry [J]. Analytical Methods, 2015, 7: 4793−4802.

Li Chaofeng, Li Xianhua, Li Qiuli, et al. Rapid and precise determination of Sr and Nd isotopic ratios in geological samples from the same filament loading by thermal ionization mass spectrometry employing a single-step separation scheme[J]. Analytica Chimica Acta, 2012, 727: 54−60.

Liu Yannan, Samaha N T, Baker D R. Sulfur concentration at sulfide saturation (SCSS) in magmatic silicate melts[J]. Geochimica et Cosmochimica Acta, 2007, 71(7): 17831−799.

Liu Yuegao, Li Wenyuan, Jia Q Z, et al. The Dynamic Sulfide Saturation Process and a Possible Slab Break-off Model for the Giant Xiarihamu Magmatic Nickel Ore Deposit in the East Kunlun Orogenic Belt, Northern Qinghai-Tibet Plateau, China[J]. Economic Geology, 2018, 113(6): 1383−1417.

Mao Jingwen, Pirajno F, Zhang Zhaochong, et al. A review of the Cu-Ni sulfide deposits in the Chinese Tianshan and Altay orogens (Xinjiang Autonomous Region, NW China): Principal characteristics and ore-forming processes[J]. Journal of Asian Earth Sciences, 2008, 32: 184−203.

Mao Qigui, Xiao Wenjiao, Windley B F, et al. Early Permian subduction-related transtension in the Turpan Basin, East Tianshan (NW China): implications for accretionary tectonics of the southern Altaids[J]. Geological Magazine, 2019. https://doi.org/10.1017/S0016756819001006.

Mao Yajing, Qin Kezhang, Tang Dongmei, et al. Crustal contamination and sulfide immiscibility history of the Permian Huangshannan magmatic Ni-Cu sulfide deposit, East Tianshan, NW China[J]. Journal of Asian Earth Sciences, 2016, 129: 22−37.

Mavrogenes J A, O'neill HSC. The relative effects of pressure, temperature and oxygen fugacity on the solubility of sulfide in mafic magmas[J]. Geochimica et Cosmochimica Acta, 1999, 63(7-8): 1173−1180.

Mc Donough W F, Sun S S. The composition of the Earth[J]. Chemical Geology, 1995, 120(3-4): 223−253.

Naldrett A J. From the mantle to the bank: the life of a Ni-Cu-(PGE) sulfide deposit[J]. South African Journal of Geology, 2010, 113: 1−32.

Pearce J A, Norry M J. Petrogenetic implications of Ti, Zr, Y and Nb variations in volcanic rocks[J]. Contrib Mineral Petrol, 1979, 69: 33−47.

Pirajno F, Mao Jingwen, Zhang Zhaochong, et al. The association of mafic-ultramafic intrusions and A-type magmatism in the Tianshan and Altay orogens, NW China: Implications for geodynamic evolution and potential for the discovery of new ore deposits[J]. Journal of Asian Earth Sciences, 2008, 32(2-4): 165−183.

Qin Kezhang, Su Benxun, Sakyi P A, et al. SIMS zircon U-Pb geochronology and Sr-Nd isotopes of Ni-Cu-bearing mafic-ultrmafic intrusions in Eastern Tianshan and Beishan in correlation with flood basalts in Tarim basin (NWChina): Constraints on a ca. 280Ma mantle plume[J]. American Journal of Science, 2011, 311(3): 237−260.

Qin K Z, Zhang L C, Xiao W J, et al. Overview of major Au, Cu, Ni and Fe deposits and metallogenic evolution of the eastern Tianshan Mountains, Northwestern China[A]. In: Mao J W, Goldfarb R J, Seltmann R, et al. (Eds.). Tectonic Evolution and Metallogeny of the Chinese Altay and Tianshan[C]. London Geological Society, 2003, 10: 227−248.

Ripley em, Li C. Sulfide saturation in mafic magmas: is external sulfur required for magmatic Ni-Cu-(PGE) ore genesis[J]. Economic Geology, 2013, 108, 45−58.

Saunders A D, Storey M, Kent R W, et al. Consequences of plume lithosphere interactions[A]. In: Storey B C, Alabaster T, Pankhurst R J (Eds.). Magmatism and the Cause of Continental Breakup[C]. London, Geological Society of Special Publication, 1992, 68: 41−60.

Shi Yu, Wang Yuwang, Wang Jingbin, et al. Physicochemical Control of the Early Permian Xiangshan Fe-Ti Oxide Deposit in

Eastern Tianshan (Xinjiang), NW China[J]. Journal of Earth Science, 2018, 29(3): 520−536.

Song Xieyan, Xie Wei, Deng Yufeng, et al. Slab break-off and the formation of Permian mafic-ultramafic intrusions in southern margin of Central Asian Orogenic Belt, Xinjiang, NW China[J]. Lithos, 2011, 127: 128−143.

Still P, Umruh D M, Tatsumoto. Pb, Sr, Nd and Hf isotopic evidence of multiple for Oahu, Hawwii basalt[J]. Nature, 1983, 304: 25−29.

Su Benxun, Qin Kezhang, Sakyi P A, et al. U-Pb ages and Hf-O isotopes of zircons from Late Paleozoic mafic-ultramafic units in the southern Central Asian Orogenic Belt: Tectonic implications and evidence for an Early-Permian mantle plume[J]. Gondwana Research, 2011, 20(2−3): 516−531.

Sun Tao, Qian Zhuangzhi, Deng Yufeng, et al. PGE and isotope (Hf-Sr-Nd-Pb) constraints on the origin of the Huangshandong magmatic Ni-Cu sulfide deposit in the Central Asian Orogenic Belt, Northwestern China[J]. Economic Geology, 2013, 108: 1849−1864.

Sun Yan, Wang Jingbin, Lv Xiaoqiang, et al. Geochronology, petrogenesis and tectonic implications of the newly discovered Cu-Ni sulfide-mineralized Yueyawan gabbroic complex, Kalatag district, northwestern Eastern Tianshan, NW China[J]. Ore Geology Review, 2019, 109: 589−614.

Tang Dongmei, Qin Kezhang, Su Benxun, et al. Magma source and tectonics of the Xiangshanzhong mafic-ultramafic intrusion in the Central Asian Oorogenic Belt, NW China, traced from geochemical and isotopic signatures[J]. Lithos, 2013, 170: 144−163.

Taylor S R, Mclennan S M. The continental crust: its composition and evolution[M]. London: Blackwell Scientific Publications, 1985, 1-312.

Wang Yuwang, Wang Jingbin, Wang Lijuan, et al. Metallogenic series related to Permian mafic complex in North Xinjiang: Post-collisional stage or mantle plume result?[J]. Acta Geologica Sinica, 2008, 82(4): 788−795.

Wendlandt R F. Sulfide saturation of basalt and andesite melts at high pressures and temperatures[J]. American Mineralogist, 1982, 67(9-10): 877−885.

Windley B F, Allen M B, Zhang C, et al. Paleozoic accretion and Cenozoic redeformation of the Chinese Tien Shan Range, Central Asia[J]. Geology, 1990, 18: 128−131.

Wykes J L, O'neill HSC, Mavrogenes J A. The Effect of FeO on the Sulfur Content at Sulfide Saturation (SCSS) and the Selenium Content at Selenide Saturation of Silicate Melts[J]. Journal of Petrology, 2015, 56: 1407−1424.

Wood D A. The application of a Th-Hf-Ta diagram to problems of tectonomagmatic classification and to establishing the nature of crustal contamination of basaltic lavas of the British Teritary volcanic province[J]. Earth and Planetary Science Letters, 1990, 50: 11−30.

Xiao Wenjiao, Windley B F, Allen M B, et al. Paleozoic multiple accretionary and collisional tectonics of the Chinese Tianshan orogenic collage[J]. Gondwana Research, 2013, 23(4): 1316−1341.

Xiao Wenjiao, Zhang Lianchang, Qin Kezhang, et al. Paleozoic accretionary and collisional tectonics of the Eastern Tianshan (China): Implications for the continental growth of central Asia[J]. American Journal of Science, 2004, 304: 370−395.

Xue Shengchao, Wang Qingfei, Deng Jun, et al. Mechanism of organic matter assimilation and its role in sulfide saturation of oxidized magmatic ore-forming system: insights from C-S-Sr-Nd isotopes of the Tulaergen deposit in NW China[J]. Mineralium Deposita, 2022, 57: 1123−1141.

Yuan Feng, Zhou Taofa, Zhang Dayu, et al. Siderophile and chalcophile metal variations in basalts: Implications for the sulfide saturation history and Ni-Cu-PGE mineralization potential of the Tarim continental flood basalt province, Xinjiang Province, China[J]. Ore Geology Reviews, 2012, 45: 5−15.

Zhao Yun, Xue Chunji, Zhao Xiaobo, et al. Variable mineraliztion processes during the formation of the Permian Hulu Ni-Cu sulfide deposit, Xinjiang, Northwestern China[J]. Journal of Asian Earth Sciences, 2016, 126: 1−13.

Zhao Yun, Liu Shengao, Xue Chunji, et al. Copper isotope fractionation in magmatic Ni–Cu mineralization systems associated with the variation of oxygen fugacity in silicate magmas[J]. Geochimica et Cosmochimica Acta, 2022, 338.

Zhou Guochao, Wang Yuwang, Shi Yu, et al. Petrogenesis and sulfide saturation of the Yueyawan Cu-Ni sulfide deposit in Eastern Tianshan, NW China[J]. Ore Geology Review. 202, 139: 104596.

Zhou Guochao, Wang Yuwang, Wang Jingbin, et al. Petrogenesis and Economic Potential of the Sangong Mafic-Ultramafic Intrusion in the Eastern Tianshan, Central Asian Orogenic Belt: Constraints from Mineral, Whole-Rock, and PGE Geochemistry[J]. Journal of Earth Science, 2024, 35: 850–865.

Zhou Meifu, Lesherr C M, Yang Z X, et al. Geochemistry and petrogenesis of 270Ma Ni-Cu-(PGE) sulfide-bearing mafic intrusions in the Huangshan district, eastern Xinjiang, northwest China: Implications for the tectonic evolution of the Central Asian orogenic belt[J]. Chemical Geology, 2004, 209(3-4): 233−257.

Zhou Meifu, Zhao Junhong, Jiang Changyi, et al. OIB-like, heterogeneous mantle sources of Permian basaltic magmatism in the western Tarim Basin, NWChina: Implications for a possible Permian large igneous province[J]. Lithos, 2009, 113: 583−594.